

Pulmonary Uptake of Technetium-99m-Sestamibi Induced by Dipyridamole-Based Stress or Exercise

Gilbert A. Hurwitz, Samia K. Ghali, Mariwan Husni, Piotr J. Slomka, Adel G. Mattar, Robert H. Reid and Neville M. Lefcoe
Departments of Diagnostic Radiology, Nuclear Medicine and Medicine, University of Western Ontario; and Department of Nuclear Medicine, Victoria Hospital, London, Ontario, Canada

On poststress images with ^{99m}Tc -sestamibi (MIBI), increased lung uptake of the radiotracer may reflect severe or multivessel coronary artery disease. **Methods:** We measured pulmonary/myocardial ratios of MIBI at standardized times on immediate poststress acquisitions and on delayed tomographic acquisitions. In 1500 sequential patients referred for rest and stress myocardial tomography, ancillary planar images were obtained 4 min postinjection at peak stress with exercise, either alone (exercise, $n = 674$), or after intravenous dipyridamole (dipyridamole, $n = 826$). **Results:** Based on 95% confidence limits in the angiographic normals, high values for immediate acquisitions were found in 17% of dipyridamole studies and 15% of exercise studies. High values for delayed acquisitions were found in 10% of dipyridamole studies and 9% of exercise studies. For both stress modes, increased values were related ($p < 0.001$) to ischemic perfusion defects for immediate images, to fixed defects for delayed images, and to ventricular dilation in both cases. By logistic regression analysis, body weight and history of infarction were also minor independent determinants ($p < 0.01$) of delayed acquisitions. In a subset of 250 cases with angiographic correlation (163 with dipyridamole; 87 with exercise), immediate lung uptake was highly correlated with ventricular dysfunction and with coronary stenoses ($p < 0.0001$). Relationships were similar to those in a historic control series imaged with ^{201}Tl . Values for delayed poststress images, and for corresponding rest images, showed strong relationships to ventricular dysfunction but not to stenosis severity. **Conclusion:** The relationships of immediate lung uptake to scintigraphic and angiographic disease patterns suggest its possible diagnostic use as an indicator of stress-induced ventricular decompensation.

Key Words: technetium-99m-sestamibi; lung uptake; tomographic acquisitions; dipyridamole

J Nucl Med 1998; 39:339-345

In using technetium-based agents for myocardial imaging (1,2), a potential drawback is the decreased value of pulmonary uptake of the perfusion agent. With ^{201}Tl , the classic radionuclide used for this purpose, lung uptake can be assessed as an ancillary aspect of interpretation of planar or tomographic imaging. Increased poststress lung uptake of ^{201}Tl has considerable diagnostic value because it correlates with multivessel or severe coronary artery disease (3-5). Major prognostic value has been attributed to this ancillary imaging sign (5-8). The diagnostic relevance of stress-induced lung uptake of ^{201}Tl has been shown after a variety of stress modalities (9,10), but relationships to gender, peak exercise heart rate and other factors may modify its interpretation (4,5). Although ^{99m}Tc -sestamibi (MIBI) has been in widespread use for several years, there is only limited information (11-15) concerning the potential value of pulmonary uptake with it. This probably derives from the standard imaging protocols with MIBI in which

imaging is usually not performed until at least 30 min after stress injection.

Published studies leave unanswered questions about the usefulness of lung uptake measurements with MIBI. On conventional MIBI images obtained 1 hr after stress, the value of lung uptake as an ancillary diagnostic sign has been reported as absent (14), reduced in comparison to ^{201}Tl (12,13) or possibly as helpful as those of ^{201}Tl (11). Most previous studies have focused on exercise rather than on pharmacological stress. Recently, Giubbini et al. (15) found that lung uptake on images acquired 1 hr after ergometric exercise correlated well with left ventricular dysfunction but not with the number of stenosed coronary arteries.

A few studies (12,13) have suggested that lung uptake of MIBI may be a more useful sign of disease when measured on immediate poststress images compared to standard acquisitions at 1 hr after injection. We reviewed the routine use of early poststress MIBI images (16) and evaluated images performed after dipyridamole-based tests as well as after ergometric stress.

MATERIALS AND METHODS

Sequential MIBI Imaging Series

From April 1992 to September 1993, 1500 sequential referrals were made to the nuclear medicine department at Victoria Hospital for diagnostic stress myocardial scintigraphy. These studies involved 1445 patients (evaluations were performed on two separate occasions in 53 patients and on three occasions in 1 patient) and were ordered by referring physicians for the usual clinical indications (16). Tomographic imaging with MIBI was used as the standard laboratory procedure to assess myocardial perfusion. Starting in April 1992, all patients had ancillary images taken starting at 4 min after peak stress with a mobile camera situated beside the stress table (13,16). These images were acquired in the left anterior oblique 40° projection for 2 min in the electrocardiogram (ECG)-gated mode with 16 frames synchronized to the R-wave. As part of routine image interpretation, these images were displayed in cinematic mode and used for visual rating of ventricular contractile function including left ventricular size (17). With all frames added together for better count statistics, these images also were used to assess abdominal background (16). Although relative lung uptake was observed on these images, quantitation of lung uptake was not included routinely.

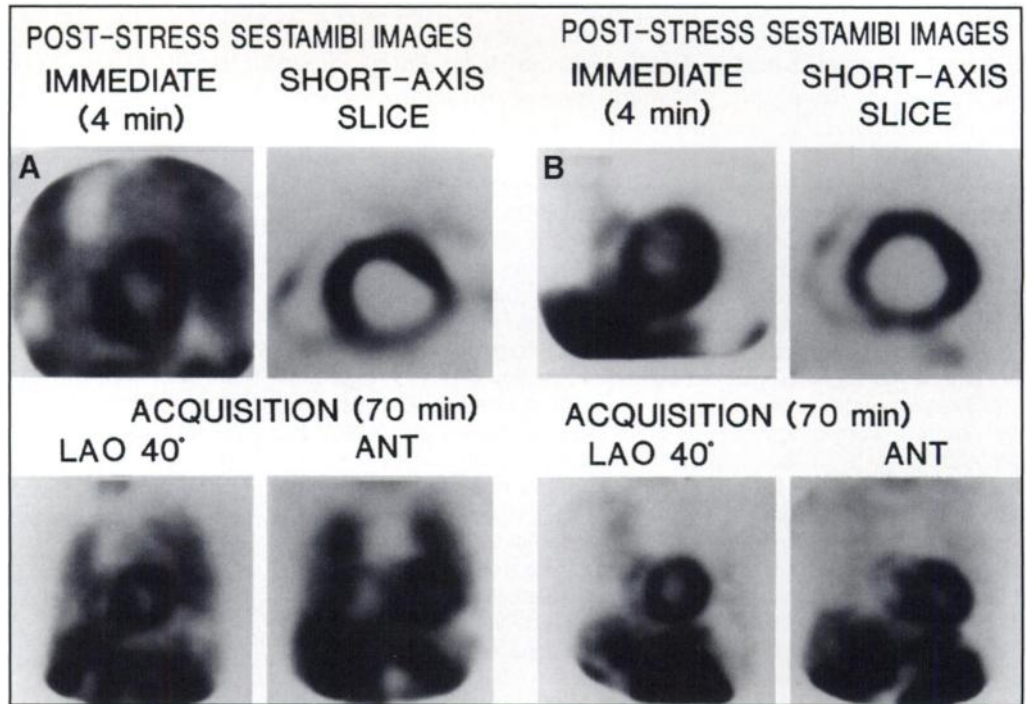
Routine MIBI Perfusion Studies

Patients were assigned to supine bicycle ergometry stress alone if a brief clinical assessment suggested that would allow them to reach a diagnostic stress level (16,18). If exercise capacity was considered limited, stress was performed with vasodilatation with dipyridamole combined with either bicycle exercise or repeated isometric exercise, as appropriate. In this series, 674 patients (45% of the 1500 patients) were studied with exercise stress alone, and 826 patients (55%) were studied with dipyridamole-based tests. At peak exercise, MIBI was injected in a dose of 12 MBq/kg body weight. To ensure MIBI uptake by the myocardium (19), exercise

Received Dec. 12, 1996; revision accepted Apr. 1, 1997.

For correspondence or reprints contact: Gilbert A. Hurwitz, MD, Department of Nuclear Medicine, Victoria Hospital, 375 South St., London, Ontario, N6A 4G5, Canada.

FIGURE 1. (A) MIBI images with stress-induced lung uptake of MIBI. This 62-yr-old man with remote bypass grafting had poor left ventricular function (ejection fraction of 36%). Upper left panel shows immediate image obtained with a mobile camera 4 min after exercise stress (6 metabolic equivalents). Ventricular dilation and increased uptake in both lungs is obvious. Lower panels (left anterior oblique 40° on left and anterior on right) show 30-sec acquisitions obtained starting 60 min after tracer injection as part of stress tomography. Upper right panel shows midventricular short-axis slice reconstructed from 32 acquisition images. Tomography showed anteroapical and infero-lateral infarcts with adjacent ischemia in a dilated left ventricle. On a subsequent study 1 yr later, performed with dipyridamole-exercise stress, lung uptake was similarly increased. (B) MIBI images in patient with normal pulmonary uptake. Image arrangement corresponds to Figure 1A. Left ventricular dilation is not present, and no perfusion defects were detected. ECG-gated blood-pool scintigraphy 5 days later showed the ejection fraction to be 24%. This 65-yr-old man with atypical chest pain and left bundle branch block exercised to a peak heart rate of 140 bpm. Correlating cardiac catheterization was consistent with idiopathic cardiomyopathy (no coronary stenoses, Grade 5 ventriculogram).



was continued after radiotracer bolus appeared in the heart as assessed on the persistence scope of the adjacent mobile camera. The peak workload was continued for 1 min followed by a wind-down period of 1.5 min. The peak exercise workload was translated into metabolic equivalents by the equation:

$$\text{METs} = (\text{kpm} \times 2 + 300) / (3.5 \times \text{kg}),$$

where kpm is the peak ergometric workload attained (16) and kg is body weight in kilograms.

Poststress tomographic imaging was performed by 180° tomography (32 stops of 30 sec) on a large field-of-view camera with stress acquisition started 1 hr after radiotracer injection. Corresponding tomographic rest images were preferentially performed on a separate day, $n = 661$ (44%), or, if required, on the same day as the stress procedure with a dose of 3 MBq/kg. After reconstruction, rest and stress images were observed in dual-display mode, cine images (17) were assessed along with relevant clinical and ECG data, and reports were generated by nuclear medicine physicians. Images were archived on optical laser disks for subsequent review.

Correlating Cardiac Catheterization

Cardiac catheterization studies were ordered by referring clinicians on clinical grounds usually after perfusion scanning. A single cardiovascular radiologist has independently reported all of our angiographic studies. Coronary stenoses were rated as a percent of luminal diameter and classified as to their position in the three main coronary arteries or branches. Left ventricular function was rated on biplane contrast ventriculography on a scale from 1 (normal) to 5 (globally hypokinetic) based on the number, site and severity of hypokinetic segments (9,20,21). On retrospective review, catheterization studies correlated to perfusion scans if (a) there was no previous revascularization, (b) infarction or revascularization did not occur between the two studies and (c) the two

diagnostic studies were performed within 4 mo of each other. Of the 1500 MIBI perfusion scans reviewed, 250 had correlating catheterization studies by these criteria.

Historical Comparison with Thallium-201 Planar Imaging

A series of 550 planar ^{201}Tl perfusion studies with correlating angiography has been described previously (16). This historical comparison series was similar to the MIBI cases with respect to selection and performance of stress tests and interpretation of correlating angiography. Angiographically correlated cases with the two agents were similar in clinical characteristics, stress-test results and incidence and severity of coronary artery disease.

Quantitation of Lung Uptake

After completing the 1500 MIBI studies, images (Fig. 1) were retrieved batch-wise from the optical disk to calculate pulmonary/myocardial ratios. ECG-gated images were initially formatted by adding all frames of the study. For MIBI images, it was essential to overcome the problem of scaling counts to variable abdominal activity (16) by finding the area of peak myocardial counts and saturating the images. Image processing was performed by two of the authors.

Regions were delineated in the myocardium and the left lung as described originally for ^{201}Tl images (18) and subsequently used for ^{201}Tl (9,20) and MIBI (13). The operator outlined a transmural segment of myocardium containing the area of peak counts (Region A) and a crescentic region over the left lung (Region B). Lung uptake was calculated as the ratios of count densities (B/A) and expressed as a percentage (Fig. 2).

In a small number of cases, images were not available or suitable for retrospective processing of lung uptake. Eleven studies were associated with low counts. Partially interstitial injection was noted during the stress procedure in five of these. In three other studies, neither immediate nor delayed poststress images were correctly

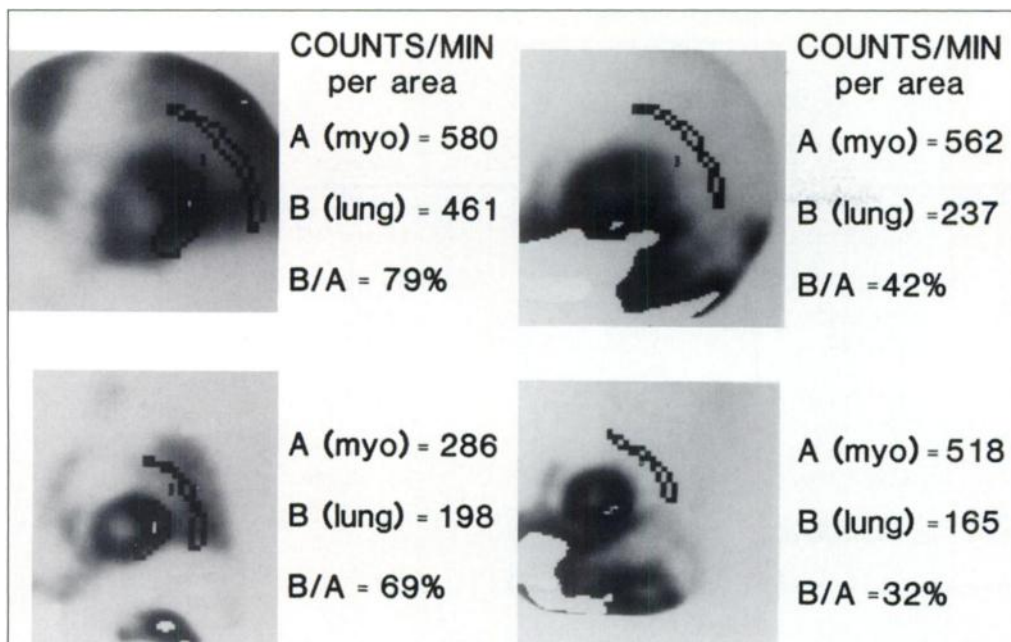


FIGURE 2. Quantitation of lung uptake of MIBI using pulmonary/myocardial ratios (P/M) in two men who had previous infarctions followed by angioplasty. Upper panels show immediate left anterior oblique 40° images and lower panels show corresponding SPECT tomographic acquisitions obtained 70 min after stress. Patient shown in left panels performed exercise to a peak heart rate of 162 bpm and had increased uptake on immediate tomographic acquisition (P/M = 69%) and on delayed tomographic acquisition (P/M = 69%). Patient on right was stressed with dipyridamole followed by a low level of exercise limited by knee pain (arthritis) and chest pain. Because of high abdominal uptake, saturation of images was necessary to visualize the myocardium, and values were within normal range on both immediate (P/M = 42%) and delayed images (P/M = 32%).

archived, and patient symptoms precluded further imaging in one. Thus, 1485 studies were suitable for further analysis:

1. Early poststress MIBI images: Of the 1485 studies, camera malfunction precluded image acquisition in six; positioning was poor in two; early poststress images were not correctly archived in five. Appropriate images could be assessed in 1472 cases.
2. Stress MIBI tomographic acquisitions: Quantitation was performed using the left anterior projection, which matched the early poststress view. The myocardium could be easily delineated on these 30-sec acquisitions, but appropriate scaling of the images was critical. Before delineation of myocardial and pulmonary regions, the left ventricle was centered in a box measuring 19×19 cm or 22% of the field of view. Planar delayed imaging, rather than tomography, was performed in four patients (due to technical or clinical limitation). Archiving deficiencies precluded data availability in 20 further studies and appropriate measurements were obtained in 1461 cases.
3. Rest MIBI tomographic acquisitions: Quantitation was performed in a similar fashion to the quantitation of stress images, but only the angiographically-correlated cases were assessed. Archived studies were available for 244 of these cases.
4. Immediate poststress ^{201}Tl images: Lung/myocardial ratios were assessed in these studies as previously described (9,20).

Review of Scintigraphic and Angiographic Data

For all studies, scintigraphic reports and hard copy of tomographic images were reviewed by one of the authors. The results of stress scintigraphic imaging studies were characterized as defect, showing a definite perfusion abnormality, dilation, showing definite left ventricular dilation on the tomograms, or normal. After a comparison of stress and rest tomograms, cases with focally abnormal perfusion were characterized further as having ischemic defects (stress > rest), fixed defects (stress = rest) or both types. Findings likely to be attributed to causes other than coronary artery disease, such as attenuation artifact or abnormal conduction (isolated septal hypoperfusion associated with left bundle branch block), were construed as normal. Although quantitation of tomographic images was not routinely performed, this evaluation was performed in a setting in which a direct method of quantitating

myocardial perfusion and left ventricular size on clinical tomograms was under development (22).

Angiographic studies were categorized according to the site and number of stenoses. For binary classification, significant disease was taken as the presence of a stenosis of at least 50% luminal diameter in one of the three main arteries (left anterior descending, right coronary and left circumflex arteries) or their branches. To calculate the number of diseased arteries, left mainstem disease was regarded as equivalent to left anterior descending plus left circumflex. A more detailed system was used to compare the effect of various arterial sites of disease to the scintigraphic findings (20). For this formulation, the left mainstem was considered a separate site, and stenoses in the left mainstem and each of the three arteries were rated on a continuous scale according to the percent of stenosis giving branch lesions half the weight of a lesion in the main arterial trunk.

Statistical Methods

Normal values for pulmonary/myocardial ratios with MIBI were calculated on the basis of catheterization data; 25 studies (11 involving dipyridamole and 14 with exercise alone) had contrast ventriculography scores of 1 (normal) and had no significant coronary artery stenoses. Upper limits of normal (95% confidence, one-tailed) were calculated for pulmonary/myocardial (P/M) ratios on immediate images and delayed images. These values were applied to the patients stressed with dipyridamole-based and exercise tests (Table 1). Characteristics of the patients having high values on the immediate images were contrasted with those having normal values. Univariate comparisons were made by paired Student's t-tests or by chi-squared tests where appropriate (Tables 2 and 3). To assess which factors might contribute independently to increased lung uptake, multivariate analysis was performed using factors identified as significant from the univariate analysis. Logistic regression analysis was performed for both stress modes and for both poststress intervals (Table 4).

In the subset of angiographically correlated cases, lung uptake values on immediate and delayed images were related to the principal angiographic findings by analysis of variance (Fig. 3). Coronary disease was tabulated as the number of diseased coronary arteries and ventricular dysfunction by the grading of contrast ventriculography. Comparison of means of specific groups was evaluated by Newman-Keuls tests.

TABLE 1
Incidence of Increased P/M Ratios on Immediate and Delayed Poststress Images*

Abnormal value	Immediate		Delayed	
	Incidence	$\geq 57\%$ p	Incidence	$\geq 46\%$ p
Scan findings				
Normal	6% (43/753)	—	2% (14/746)	—
Single findings				
Ischemic defects (I)	19% (40/209)	‡	9% (18/205)	‡
Fixed defects (F)	14% (18/127)	†	10% (13/127)	‡
Dilated ventricle (D)	21% (7/34)	†	9% (3/35)	†
Combined findings				
I + F	24% (29/122)	‡	20% (25/123)	‡
I + D	33% (9/27)	‡	11% (3/27)	†
F + D	41% (33/80)	‡	34% (27/79)	‡
I + F + D	46% (55/120)	‡	34% (41/119)	‡

*These images are the results of rest/stress per fusion tomography.

†p < 0.01.

‡p < 0.001 by chi-squared tests in comparison with the group with normal perfusion tomography.

P/M = pulmonary/myocardial ratio.

Further modeling of the angiographic correlates of pulmonary/myocardial ratios was then performed. As similar values and influences were previously shown for the two stress-mode groups (Fig. 3), they were pooled for this purpose. Multilinear relationships were derived for dependence on the severity of stenoses at four sites (the left mainstem and each of the three principal coronary arteries) and on contractile dysfunction (Table 5). The resulting coefficients for sites of stenosis indicate the magnitude and statistical significance of the effect of a 100% stenosis at each site. The coefficient for contractile dysfunction indicates the effect of the poorest level of function (Grade 5 by contrast ventriculography) on pulmonary/myocardial ratios. As the effect of stenoses on flow likely was related to obstructed arterial area, the square of the obstructed luminal diameter was used for modeling. Use of this function improved correlations in comparison to a linear model or to several nonlinear models. Similar analyses were performed for the rest MIBI studies and for the historic ²⁰¹Tl controls.

TABLE 2

Dipyridamole-Based Scintigraphic Studies: Characteristics of Patients According to the Value of Immediate Poststress Lung Uptake (normal $\leq 56\%$)

Characteristic	High P/M	Normal P/M	P value*
	n=139	n=678	
Gender (male)—%	71%	52%	<0.001
Age (yr)—mean \pm s.d.	61 \pm 10	61 \pm 11	0.9
Weight (kg)—mean \pm s.d.	86 \pm 17	79 \pm 16	<0.001
Revascularization—%	25%	22%	0.4
Infarction (by history)—%	65%	34%	<0.001
Hypertension—%	53%	46%	0.3
Workload (METs)—mean \pm s.d.	3.8 \pm 1.6	4.2 \pm 1.9	0.04
Peak heart rate (bpm)—mean \pm s.d.	107 \pm 20	112 \pm 20	0.01
Protocol (same day)—%	55%	57%	0.7
Scan findings†—%			
Ischemic defects	61%	33%	<0.001
Fixed defects	65%	29%	<0.001
Ventricular dilation	51%	15%	<0.001

*Chi-squared or t-tests as appropriate.

†Presence of findings either alone or in combination.

P/M = pulmonary/myocardial ratio.

RESULTS

Increased lung uptake was found on early poststress MIBI images relatively frequently in our referred population (Table 1). Values greater than 56% on the immediate images were found in 16% of the evaluable images. There was no difference between the test modes in this regard (p = 0.8 by chi-squared testing). High values were associated with ischemic defects, with fixed defects and left ventricular dilation, but they were most common when several of these abnormal findings were present. In contrast, among those with normal tomograms, the incidence of high lung ratios (6%) was similar to that among the angiographically-defined normals.

On delayed images, values for lung uptake were lower and generally correlated with immediate values (delayed = 0.69 \times immediate; r = 0.814, p < 0.0001). Increased values for lung uptake on the delayed images were less frequent than for the immediate poststress images (234/1472 versus 144/1461, p < 0.0001) across the spectrum of tomographic results (Table 1); in

TABLE 3

Exercise Scintigraphic Studies: Characteristics of Patients According to the Value of Immediate Poststress Lung Uptake

Characteristic	High P/M	Normal P/M	P value*
	n = 95	n = 560	
Gender (male)—%	79%	69%	0.05
Age (yr)—mean \pm s.d.	56 \pm 9	56 \pm 11	0.9
Weight (kg)—mean \pm s.d.	85 \pm 14	80 \pm 15	0.01
Revascularization—%	29%	24%	0.3
Infarction (by history)—%	43%	26%	<0.001
Hypertension—%	29%	31%	0.7
Workload (METs)—mean \pm s.d.	6.4 \pm 1.8	7.1 \pm 1.9	<0.001
Peak heart rate (bpm)—mean \pm s.d.	134 \pm 20	139 \pm 20	0.04
Protocol (same day)—%	57%	55%	0.7
Scan findings†—%			
Ischemic defects	51%	22%	<0.001
Fixed defects	47%	22%	<0.001
Ventricular dilation	35%	9%	<0.001

*Chi-squared or t-tests as appropriate.

†Presence of findings either alone or in combination.

P/M = pulmonary/myocardial ratio.

TABLE 4

Factors Contributing to Increased Lung Uptake on Immediate Poststress and Delayed Tomographic Images

Images	Dipyridamole-based		Exercise alone	
Immediate	Ischemic defect	‡	Ischemic defect	‡
	Dilation	‡	Dilation	‡
	Body weight	‡		
Delayed	Fixed defect	‡	Fixed defect	‡
	Dilation	‡	Dilation	‡
	Body weight	†	Ischemic defect	†
	Infarction	†		

*These table findings are the results of multifactorial logistic regression analysis.

†p < 0.01.

‡p < 0.001.

particular, a weaker association with ischemic defects was suggested. Figure 1A shows concordant elevated values for the immediate and delayed images (80% and 64%, respectively),

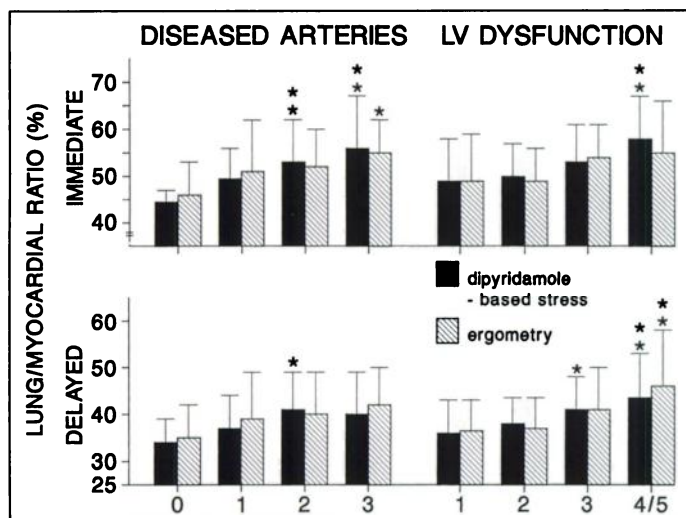


FIGURE 3. Lung/myocardial ratios (mean ± s.d.) on immediate and delayed poststress images according to dipyridamole use in scintigraphic stress imaging protocol and angiographic findings. Studies were grouped according to number of diseased coronary arteries (minimum 50% stenosis) in left panel, and according to grading of ventricular function on biplane contrast ventriculography (1 = normal, 5 = globally hypokinetic) in right panel. Increased values are shown compared to normal group (no coronary stenoses or normal ventricular function): * p < 0.05; ** p < 0.01.

and Figure 1B shows concordant normal values (48% and 37%, respectively).

High initial lung uptake (Tables 2 and 3) was found more often in those with a history of infarction and in those showing significant abnormalities on subsequent tomographic images. Such studies were not distinguished from those with normal values by age, frequency of prior revascularization or by hypertension. These relationships of increased lung uptake were generally similar on exercise and on dipyridamole-based tests. However, the association of increased lung uptake with male gender and with increased body weight seemed more prominent on the pharmacological stress tests. The relationship with attained workload was more prominent on the exercise tests. Multivariate analysis suggested (Table 4) that tomographic imaging findings were the major determinants of increased lung uptake and that clinical and stress-mode factors played minor roles. Obesity seemed to be a factor independently associated with increased lung uptake, as it was observed in some cases with presumed false-positive lung uptake measurements i.e. normal tomographic results.

Table 4 displays the contrasts between immediate and delayed lung uptake measurements with respect to associated scintigraphic findings. For the immediate images, ischemic defects provided a major independent contribution. In contrast, fixed defects were noncontributory. For the delayed images, fixed defects contributed to a much greater extent than did ischemic defects. Ventricular dilation played a major role as a synergistic contributor in both circumstances. There was a notable similarity of findings in this regard between the pharmacologically enhanced and exercise stress modes.

In the angiographic series (Fig. 3), mean values for immediate lung uptake reflected the extent of coronary artery disease increasing from 46% in those without significant stenoses to 56% in those with triple-vessel disease. Values also increased in relation to dysfunction shown on contrast ventriculography. By analysis of variance, the overall effect on the immediate ratio of coronary stenosis extent (F = 10, p < 0.0001) was greater than that of ventricular dysfunction (F = 7, p = 0.0002). The effect on the delayed ratio was greater for ventricular dysfunction (F = 11, p < 0.0001) than for extent of stenosis (F = 6, p = 0.0004). The pattern was similar for dipyridamole-based and for ergometric stress tests as substantiated by analysis of interaction terms. Despite these consistent patterns for group means, there was considerable variation among individuals. Figure 4 shows the range of immediate lung uptake values in men with significant coronary stenoses and normal ventricular function.

TABLE 5

Multivariate Regression Equations Linking Lung Uptake of Myocardial Perfusion Agents with Angiographic Features

Agent	State	Time	Equation
MIBI*		Immediate	P/M = 45 + 14 LM + 8 LAD + 3 RCA + 2LCX + 5 CD
MIBI	Stress	Delayed	P/M = 34 + 15 LM + 4 LAD + 2 RCA + 2LCX + 8 CD
MIBI	Rest	Delayed	P/M = 38 + 1LM + 0LAD + 2RCA + 0LCX + 6 CD
²⁰¹ Tl†	Stress	Immediate	P/M = 43 + 11 LM + 7 LAD + 2RCA + 1LCX + 9 CD

*N = 250 for MIBI.

†N = 550 for ²⁰¹Tl.

Statistically significant contribution indicated by bold where p < 0.05 and by underline where p < 0.001. Angiographic features are scaled from 0 (no disease) to 1 (100% stenosis, grade 5/5 ventricular dysfunction); stenosis severity is entered as the square of the obstructed luminal diameter. P/M = pulmonary/myocardial ratio (%); LM = left mainstem stenosis; LAD = left anterior descending artery stenosis; RCA = right coronary artery stenosis; LCX = left circumflex artery stenosis; CD = contractile dysfunction by ventriculography.

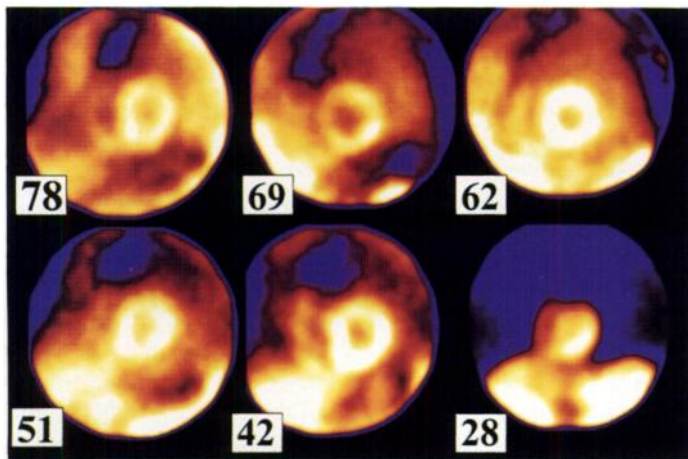


FIGURE 4. Examples of immediate (4-min) poststress images with ^{99m}Tc -MIBI in angiographically correlated studies showing the range of lung uptake. All cases were men with normal biplane contrast ventriculograms and significant coronary artery lesions (all had at least 70% stenosis in left anterior descending artery). To show relative lung uptake, each image is saturated to peak activity in myocardium. Lung uptake values (lung/myocardial ratios) are shown in lower left corner.

In these same cases, delayed images gave lung uptake values ranging from 62% (upper left) to 19% (lower right).

The multifactorial regression models shown in Table 5 indicate the relationship of lung uptake ratios, measured under differing physiological and imaging conditions, to specific sites of arterial stenosis as well as to ventricular dysfunction. Relationships of lung uptake on early poststress MIBI images were similar to those of ^{201}Tl . With both perfusion agents, left mainstem and left anterior descending artery stenoses were the main lesions contributing to pulmonary uptake modified by left ventricular function. Other sites of stenosis provided only minor contributions to lung uptake ratios in this paradigm. On the corresponding rest tomographic acquisitions, left ventricular dysfunction contributed to lung uptake whereas coronary stenoses did not. The delayed poststress images were influenced to a greater extent by ventricular dysfunction than by stenosis severity.

DISCUSSION

Our study suggests the feasibility and potential diagnostic value of routine assessment of lung uptake of MIBI on immediate poststress images. Imaging was started 2.5 min after completion of the wind-down phase of the stress procedure (16,19) with satisfactory data obtained in over 98% of cases. The allocation of a mobile gamma camera to acquire these ancillary images in the stress laboratory may have other advantages. Such a camera may be used to obtain first-pass ventriculographic studies (15,23) and to ensure adequate myocardial uptake of the radiotracer from the blood pool before exercise is stopped (19). With the patient connected to monitoring leads in the immediate poststress period, electrocardiographic gating of the early poststress images can be accomplished easily (17,21) and ventricular contractile function assessed. In cases with severe coronary artery disease, such images may reveal stress-induced ventricular dilation or dyskinesis (24) as well as stress-induced lung uptake.

Analysis of the frequency and relationships of data derived from early and delayed poststress imaging (Tables 1 and 5, Fig. 3) confirms that lung uptake with MIBI may have important diagnostic value when measured on immediate poststress images (12,13). Some investigators have found relatively poor relationships between lung uptake and coronary stenoses when

measured on MIBI tomographic acquisitions at 1 hr after stress injection (13–15). Giubbini et al. (15) found inverse relationships between left ventricular ejection fraction measured on first-pass studies and delayed measurements. This study (Fig. 3 and Table 5) supports the findings of Giubbini et al. (15) by documenting a strong relationship of delayed lung uptake measurements (both rest and stress) to left ventricular dysfunction as assessed by contrast ventriculography. Measurements obtained early poststress in our study, but not those obtained under other physiologic conditions, were strongly correlated with the extent and severity of coronary disease. These findings are not unexpected given the tendency for rapid clearance from the lung of both ^{201}Tl (25) and MIBI (13). Depending on the diagnostic objectives and the equipment available, quantitation of lung uptake on either immediate or delayed MIBI images could be of value.

The angiographic relationships of early poststress lung uptake of MIBI, including the importance of coronary stenoses, parallel those with ^{201}Tl . Although others have emphasized the relationship of increased lung uptake to multivessel disease, our results show the predominance of stenoses along the left axis (20), left mainstem or left anterior descending arteries with both radiotracers (Table 5) in induction. Our results (Fig. 3) suggest a similar interpretation of lung uptake for MIBI whether stress is performed with vasodilators or with exercise alone. Our results in normal patients differ from that of the Montreal group (26), which is probably due to the nature of our subjects.

The findings of our study may not apply uniformly to other laboratories performing rest or stress perfusion studies with MIBI. As initial and delayed MIBI images frequently show high abdominal uptake (16), proper scaling of the digitized images (to the peak area of uptake in myocardium) needs to be performed. Duplication of our results by other centers will require attention to this preliminary step in processing. In our laboratory, the particular stress modality used did not significantly affect the frequency of increased lung uptake, but this finding requires verification by centers where stress is performed with other protocols. Our experience suggests that outlining the inferior myocardium may be difficult and may lead to errors in assessing lung uptake ratios when dipyridamole is used without supplementary exercise. When upright exercise on a treadmill or bicycle is used, P/M ratios may well have lower values. Earlier acquisition of tomographic images (30 min poststress) might improve the relationship of lung uptake to coronary stenoses.

Further limitations of our study need to be addressed before recommending routine assessment of immediate poststress MIBI images. In the minutes after injection, MIBI undergoes more dynamic change than is the case with ^{201}Tl (13,19). The optimal window for assessing lung activity of MIBI might best be determined with a high-count multicrystal camera, which also would allow careful simultaneous definition of the relation with parameters of left ventricular function. The prognostic implications of increased MIBI lung uptake will need to be evaluated and compared to those of ^{201}Tl . Lung uptake varies widely among patients who are similar with respect to left ventricular function (Fig. 1, reduced function; Fig. 4, normal function). A larger number of patients will need to be evaluated to compare lung uptake with other prognostic indicators.

CONCLUSION

Increased lung uptake on immediate (4-min) poststress images with MIBI is seen in a significant portion of studies with abnormalities on perfusion tomograms. This potential ancillary diagnostic sign appears related to ischemic perfusion defects,

may be induced with exercise alone or with dipyridamole-based stress, and it is seen more frequently with severe disease. In a subset of MIBI studies with correlating angiograms, relationships to coronary artery stenoses were similar to those of ^{201}Tl . By comparison, lung uptake on delayed (1-hr) MIBI images is less frequent, and it appears related to fixed defects and to poor ventricular function. Further investigation of the potential value of early poststress MIBI images may result in the recovery of an important ancillary diagnostic sign, which appears to have been lost with the transition from ^{201}Tl - to $^{99\text{m}}\text{Tc}$ -based perfusion agents.

ACKNOWLEDGMENTS

We thank the Visual Services Department of Victoria Hospital for preparing the figures, Ms. Soraya Ali, Ms. Judy Smith and Mrs. Jo-Anne Quann for secretarial support. We also thank Dr. Craig A. MacDonald, who, until his retirement in December 1995, reported all cardiac catheterization studies at our hospital.

REFERENCES

1. Wackers FJT, Berman DS, Maddahi J, et al. Technetium-99m hexakis 2-methoxyisobutyl isonitrile: human biodistribution, dosimetry, safety and preliminary comparison to thallium-201 for myocardial perfusion imaging. *J Nucl Med* 1989;30:302-311.
2. Leppo JA, DePuey EG, Johnson LL. A review of cardiac imaging with sestamibi and teboroxime. *J Nucl Med* 1991;32:2012-2022.
3. Boucher CA, Zir LM, Beller GA, et al. Increased lung uptake of thallium-201 during exercise myocardial imaging: clinical hemodynamic and angiographic implications in patients with coronary artery disease. *Am J Cardiol* 1980;46:189-196.
4. Kaul S, Chesler DA, Boucher CA, Okada RD. Quantitative aspects of myocardial perfusion imaging. *Semin Nucl Med* 1987;17:131-144.
5. Mahmood S, Buscombe JR, Ell PJ. The use of thallium-201 lung/heart ratios. *Eur J Nucl Med* 1992;19:807-814.
6. Gill JB, Ruddy TD, Newell JB, Finkelstein DM, Strauss HW, Boucher CA. Prognostic importance of thallium uptake by the lungs during exercise in coronary artery disease. *N Engl J Med* 1987;317:1486-1489.
7. Miller DD, Kaul S, Strauss HW, Newell JB, Okada RD, Boucher CA. Increased exercise thallium-201 lung uptake: a non-invasive prognostic index in two-vessel coronary artery disease. *Can J Cardiol* 1988;4:270-276.
8. Pollock SG, Abbott RD, Boucher CA, Beller GA, Kaul S. Independent and incremental prognostic value of tests performed in hierarchical order to evaluate patients with suspected coronary artery disease. *Circulation* 1992;85:237-248.
9. Hurwitz GA, O'Donoghue JP, Powe JE, Gravelle DR, MacDonald AC, Finnie KJC. Pulmonary thallium-201 uptake following dipyridamole-exercise combination compared with single modality stress-testing. *Am J Cardiol* 1992;69:320-326.
10. Villanueva FS, Kaul S, Smith WH, Watson DD, Varma SK, Beller GA. Prevalence and correlates of increased lung/heart ratio of thallium-201 during dipyridamole stress imaging for suspected coronary artery disease. *Am J Cardiol* 1990;66:1324-1328.
11. Maisey MN, Mistry R, Sowton E. Planar imaging techniques used with technetium-99m sestamibi to evaluate chronic myocardial ischemia. *Am J Cardiol* 1990;66:47E-54E.
12. Taillefer R, Costi P, Jarry M, Benjamin C, Leveille J, Lambert R. Increased $^{99\text{m}}\text{Tc}$ -sestamibi (MIBI) lung uptake in diagnosis of coronary artery disease: comparison between early (5 min) and delayed (60 min) post-stress MIBI and ^{201}Tl planar imaging [Abstract]. *J Nucl Med* 1993;34(suppl):121P.
13. Hurwitz GA, Fox SP, Driedger AA, Willems C, Powe JE. Pulmonary uptake of sestamibi on early post-stress images: angiographic relationships, incidence and kinetics. *Nucl Med Commun* 1993;14:15-22.
14. Saha M, Forrest, TF, Brown KA. Lung uptake of technetium-99m sestamibi: relation to clinical, exercise, hemodynamic, and left ventricular function variables. *J Nucl Cardiol* 1994;1:52-56.
15. Giubbini R, Campini R, Milan E, et al. Evaluation of technetium-99m-sestamibi lung uptake: correlation with left ventricular function. *J Nucl Med* 1995;36:58-63.
16. Hurwitz GA, Saddy S, O'Donoghue JP, et al. The VEX-test for myocardial scintigraphy with Tl-201 and sestamibi: effect on abdominal background activity. *J Nucl Med* 1995;36:914-920.
17. Hurwitz GA, Powe JE, Melendez L, Ali SA, Lim RK, Miller DB. Equilibrium wall motion studies with sestamibi: evaluation of parameters for routine acquisition [Abstract]. *Clin Nucl Med* 1995;20:656.
18. Hurwitz GA, Powe JE, Driedger AA, Finnie KJC, Laurin NR, MacDonald AC. Dipyridamole combined with symptom-limited exercise for myocardial perfusion scintigraphy: image characteristics and clinical role. *Eur J Nucl Med* 1990;17:61-68.
19. Hurwitz GA, Blais M, Powe JE, Champagne CL. Stress/injection protocols for myocardial scintigraphy with sestamibi and thallium-201: implications of early post-stress kinetics. *Nucl Med Commun* 1996;17:400-409.
20. Hurwitz GA, MacDonald AC. Stenoses of the left anterior descending artery: predominant role in stress-induced pulmonary uptake of thallium-201. *Can J Cardiol* 1994;10:982-988.
21. Hurwitz GA, Laurin NR, Powe JE, Driedger AA, MacDonald AC. Ischemic left ventricular dysfunction assessed on ECG-gated thallium-201 myocardial perfusion images. *Can J Cardiol* 1990;6:198-204.
22. Slomka PJ, Hurwitz GA, St Clement G, Stephenson J. Three-dimensional demarcation of perfusion zones corresponding to specific coronary arteries: application for automated interpretation of myocardial SPECT. *J Nucl Med* 1995;36:2120-2126.
23. Hurwitz GA, Babensee SE, Craddock TD, Powe JE, Driedger A. Simplified first-pass technique for left ventricular ejection fraction with rest/stress myocardial perfusion imaging [Abstract]. *Eur J Nucl Med* 1990;16:55.
24. Hurwitz GA, O'Donoghue JP, MacDonald AC, Laurin NR, Powe JE. Markers of left ventricular dysfunction induced by exercise, dipyridamole or combined stress on ECG-gated myocardial perfusion scans. *Nucl Med Commun* 1993;14:318-327.
25. Rothendler JA, Boucher CA, Strauss HW, Pohost GM, Okada RD. Decrease in the ability to detect elevated lung thallium due to delay in commencing imaging after exercise. *Am Heart J* 1985;110:830-835.
26. Primeau M, Taillefer R, Essiambre R, Lambert R, Honos G. Technetium-99m sestamibi myocardial perfusion imaging: comparison between treadmill, dipyridamole and trans-oesophageal atrial pacing "stress" tests in normal subjects. *Eur J Nucl Med* 1991;18:247-251.